Since January 2020 Elsevier has created a COVID-19 resource centre with free information in English and Mandarin on the novel coronavirus COVID-19. The COVID-19 resource centre is hosted on Elsevier Connect, the company's public news and information website.

Medical Engineering and Physics 98 (2021) 36–43

Contents lists available at ScienceDirect

Medical Engineering and Physics

journal homepage: www.elsevier.com/locate/medengphy

The effects of face mask specifications on work of breathing and particle filtration efficiency

Mojdeh Monjezi , Hamidreza Jamaati *

Chronic Respiratory Diseases Research Center (CRDRC), Critical Care Department Shaheed Bahonar Ave., National Research Institute of Tuberculosis and Lung Diseases (NRITLD), Masih Daneshvari Hospital, Shahid Beheshti University of Medical Sciences, Darabad, Tehran 1955841452, Iran

ARTICLE INFO

Keywords:
Work of breathing (WOB)
Particle filtration efficiency (PFE)
Porosity
Fiber diameter
Filtering facepiece respirator (FFR)
Surgical face mask (SM)
Most penetrating particle size (MPPS)
Respiratory protective device (PRD)

ABSTRACT

The outbreak of the ongoing coronavirus disease 2019 (COVID-19) pandemic has led to the recommended routine use of face masks to reduce exposure risk. In this study, the increase in work of breathing (WOB) imposed by face masks is theoretically studied for both normals and patients with obstructive and restrictive lung diseases at different levels of activity. The results show a significant increase in WOB due to face masks, which is more severe in higher activity levels. The added WOB is considerable during physical activity and may be intolerable for patients with preexisting lung disease and may contribute to inspiratory muscle fatigue and dyspnea. Moreover, in this study, the effects of the physical properties of a fibrous medium, including thickness, porosity, and fiber diameter, are analyzed on the particle filtration efficiency (PFE) and the added WOB. The relations between the physical properties of the fibrous medium and the added WOB and the PFE are shown on some contour plots as a quick and simple tool to select the desired physical properties for a single layer filter to ensure that the added WOB is comfortable while the PFE is sufficiently high.

1. Introduction

Since the emergence of the ongoing coronavirus disease 2019 (COVID-19) pandemic, the routine use of respiratory protective devices (RPDs) has been recommended to reduce exposure risk. Furthermore, the most recent recommendations of the World Health Organization include the wearing of face masks by the general public for mitigating the risk and impact of COVID-19. The most used RPDs among healthcare workers and the general population are surgical face masks (SMs) and filtering facepiece respirators (FFRs), especially N95 FFRs. The continual wearing of RPDs is crucial for personal protection from exposure to contaminated particles or the risk of respiratory infections. Although RPDs are mandatory and highly recommended for areas most affected by the COVID-19 pandemic, significant difficulties have been observed in RPD wearers because of physical symptoms and discomfort.

Major experimental studies have been performed on PRDs comfortability. Some researchers used automated breathing and metabolic simulators [1,2], while others tested the masks comfortability on human subjects [3,4]. Potential reasons for discomfort with masks include a high temperature in the mask cavity leading to thermal discomfort [3–8], CO_2 accumulation, decreased oxygen causing headaches while wearing N95 FFRs [1,6,9], and mechanical factors such as increased breathing resistance [2,4,6]. A recent study has shown that panic-prone individuals may be at higher risk of mask-related respiratory discomfort [10].

An increase in breathing resistance up to approximately 300% for N95 FFRs was previously reported [4]. The increased breathing resistance, in association with CO_2 rebreathing while wearing masks, may amplify respiratory fatigue and impair physical work capacity [11]. However, no indications of increased respiratory effort at a low workload for a relatively brief period were observed by Roberge et al. [12]. Hopkins et al. reported that the pulmonary function and cardiopulmonary exercise capacity highly impaired by N95 FFRs in healthy individuals [13]. Later, Hopkins et al. found some flaws in their work which took the validity of the study into question [13]. The authors discussed that since there were no significant different results for arterial blood gasses, heart rate, cardiac output and blood pressure between masked and unmasked conditions, in no way should it serve as a recommendation for avoiding mask use during exercise. These different results suggest the use of a mathematical model to investigate the effect of workload level on the increased work of breathing (WOB).

There are various experimental researches in the context of particle filtration efficiency (PFE) of face masks [14–16]. Well-fitted respirators

* Corresponding author.
E-mail address: hamidjamaati@hotmail.com (H. Jamaati).

https://doi.org/10.1016/j.medengphy.2021.10.004
Received 14 July 2021; Received in revised form 1 October 2021; Accepted 4 October 2021
Available online 6 October 2021

Nomenclature

Symbol description units

ΔPpressure drop pressure dropPa
∇Ppressure gradient pressure gradientPa.m^{-1}
μdynamic viscosity of the air dynamic viscosity of the airPa.s
*A*surface area of pore section surface area of pore sectionm^2
C_{rs}respiratory compliance respiratory compliancem^3.Pa^{-1}
C_sCunningham slip correction factor Cunningham slip correction factor-
*D*diffusion coefficient of particle diffusion coefficient of particlem^2.s^{-1}
$d_f$fiber diameter fiber diameterm
$d_p$particle diameter particle diameterm
*f*air flow rate air flow ratem^3.s^{-1}
*F*forchheimer coefficient forchheimer coefficient-
*k*permeability coefficient permeability coefficientm^2
$k_B$boltzmann constant boltzmann constantj.K^{-1}
Knknudsen number of particle knudsen number of particle-
Kukuwabara hydrodynamic factor kuwabara hydrodynamic factor-
*L*filter thickness filter thicknessm
Pepeclet number of particle peclet number of particle-
*R*interception parameter interception parameter-
RRbreathing frequency breathing frequencymin^{-1}
Re_pparticle Reynolds number particle Reynolds number-
R_{rs}respiratory resistance respiratory resistancePa.s.m^{-3}
Stkstokes number stokes number-
*T*absolute temperature absolute temperatureK
$t_i$inspiration time inspiration times
*v*face velocity face velocitym.s^{-1}
$V_T$tidal volume tidal volumem^3
W_{mask}added WOB due to mask resistance added WOB due to mask resistancej

Greek letters

*A*solidity of the filter medium solidity of the filter medium-
*E*porosity of the filter medium porosity of the filter medium-
ηPFE of the fibrous medium PFE of the fibrous medium-
η_APFE of the single fiber due to adhesion PFE of the single fiber due to adhesion-
η_DPFE of the single fiber due to diffusion PFE of the single fiber due to diffusion-
η_fPFE of the single fiber PFE of the single fiber-
η_IPFE of the single fiber due to inertial impaction PFE of the single fiber due to inertial impaction-
η_RPFE of the single fiber due to interception PFE of the single fiber due to interception-
λmean free path of air molecules mean free path of air moleculesm
ρdensity of the polypropylene density of the polypropylenekg.m^{-3}
ρ_{SF}surface density of the filter medium surface density of the filter mediumkg.m^{-2}
Φdimensionless pressure drop dimension -less pressure drop-

Table 1
Physical characteristics of the N95 FFR1.

Layer	Thickness (mm)	Fiber diameter (μm)	Packing density (α)	Surface area (m^2)
External	2.27	22.1	0.104	0.0163
Middle	1.77	5.4	0.096	
Internal	0.36	15.4	0.101	

are required to achieve > 95% aerosol filtration under standard conditions. PFE depends on the filter material [17,18], the properties of the fibers, including structure, diameter and electrostatic charges [17, 19–21], the number of layers [22], shape (surgical style, conical, or duckbill), and facial fit [17,23,24]. Moreover, a considerable reduction in PFE during a cyclic coughing incident has been observed [25]. Although the main mechanisms for aerosol penetration through the masks are well studied [26], the combined effects of physical properties of the fibrous medium (including fiber diameter, porosity, and thickness) and the wearer's level of activity on PFE are not reported.

This study computes the increase in WOB imposed by masks through a porous media model. Then, the effects of physical properties of the fibrous medium and the wearer's level of activity are investigated on the added WOB and the PFE.

2. Material and methods

The filter medium, made up of randomly-oriented fibers, was defined as a porous media to simulate its resistance to flow. Assuming an adequate fit condition, almost all inhaling air passes through the filter medium without leakage. In laminar flow through porous media, the pressure drop is proportional to velocity according to Darcy's law [27]:

$$\nabla P = -\frac{\mu}{k} v \tag{1}$$

In this equation, v is the face velocity, k is the permeability coefficient of the medium, and μ is the dynamic viscosity of the fluid (1.8e-5 Pa.s), and ∇P is the pressure gradient in the thickness of the medium, L.

The face velocity is the fluid velocity and is related to the fluid flow rate, f, through the Eq. (2).

$$v = \frac{f}{A} \tag{2}$$

in which, A is the surface area of the filter medium. According to detailed physical properties found in the literature for classical surgical masks [28], we have found the solidity of surgical masks using Eq. (3).

$$\alpha = \frac{\rho_{SF}}{L\rho} \tag{3}$$

where ρ_{SF} is the surface density and ρ is the available density of the polypropylene [29]. So, the assumed porosity of the surgical mask, ε =1-α, is 0.71.

For N95 FFRs, we have used the previously reported values for the physical characteristics of the N95 3M8510 (FFR1) listed in Table 1 [30], while for the surgical mask such data were not available. For the surgical mask, the reported pressure drop were 2.667 ± 0.137 mmH2O with the KFDA protocol (constant flow rates of 30 l/min) [24]. Substitution into Eq. (1) gives the average air permeability of 4.84e-12 m^2. The assumed surface area and thickness of surgical mask is 163 cm^2 [31] and 0.234 mm [28], respectively.

According to the theoretical predictions of Spielman and Goren [32], dimensionless pressure drop, Φ, can be expressed by the following curve-fitted equation for the case in which all fibers are normal to flow direction.

$$\Phi = \frac{\Delta P.d_f^2}{16\alpha\mu v L} = \frac{d_f^2}{16k\alpha} = 372.8\alpha^3 - 66\alpha^2 + 14\alpha + 0.315 \tag{4}$$

in which α is the solidity or packing density of the fiber medium. So, the permeability of each layer of the N95 FFR can be computed by Eq. (5).

Table 2
Breathing parameters assumed in different levels of activity.

	Rest	light activity	moderate activity	heavy activity
Minute ventilation (l/min)	15	30	60	85
RR (cycle/min)	15	25	30	35
V_T (l)	1.00	1.20	2.00	2.43
t_i (s)	1.80	1.08	0.90	0.77
Flow rate (l/s)	0.56	1.11	2.22	3.15

Table 3
Formulations of the PFE of a single fiber by different mechanisms; inertial impaction, diffusion and adhesion.

Inertial impaction	$\eta_I = \frac{2R(1-\alpha)Stk\sqrt{\alpha} + (1-\alpha)\alpha Stk^2}{ku}$	[40]
Interception	$\eta_R = \frac{1+R}{2ku}\left(2\ln(1+R) - 1 + \alpha + \left(\frac{1}{1+R}\right)^2\left(1 - \frac{\alpha}{2}\right) - \frac{\alpha}{2}(1+R)^2\right)$	[41]
Diffusionz	$\eta_D = 2.9Ku^{-1/3}Pe^{-2/3} + 0.62Pe^{-1}$	[42]
Adhesion	$\eta_A = \frac{190}{(Re_p * Stk)^{0.68} + 190}$	[43]
Governing parameters	$R = \frac{d_p}{d_f}$	
	$Stk = \frac{dp^2\rho_p Cs\, v}{18\mu d_f}$	
	$ku = -\ln(\alpha)/2 + \alpha - \alpha^2/4 - 3/4Kn = \frac{2\lambda}{d_p}Pe = \frac{v.d_f}{D}D = \frac{k_B TC_s}{3\pi\mu d_p}C_s$	
	$= 1 + Kn\left(1.207 + 0.44exp\left(-\frac{0.78}{kn}\right)\right)Re_p = \frac{\rho_p d_p v}{\mu}$	

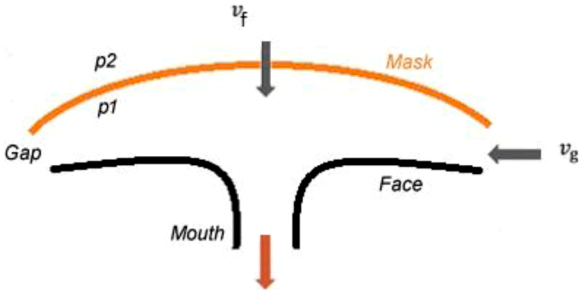

Fig.1. Schematic of mask with face-seal leakage [44].

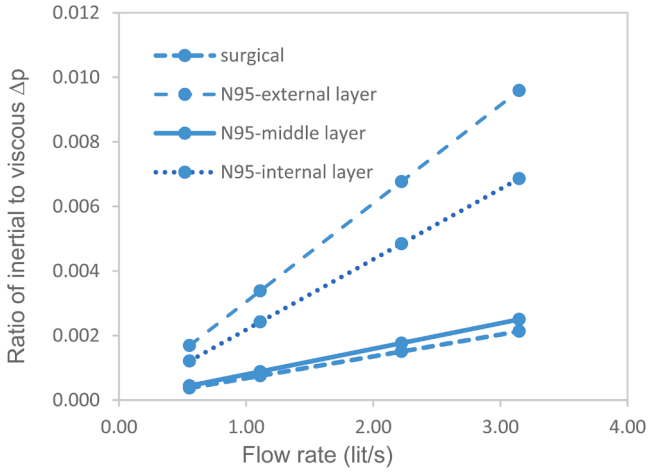

Fig.2. The importance of considering F coefficient in pressure drop of face masks.

Table 4
Effect of wearing surgical masks and N95 respirators without leakage on the pressure drop, resistance, and WOB at different levels of activity.

Surgical mask				
Level of activity	Rest	Light	Moderate	Heavy
Pressure drop (cmH2O)	0.30	0.59	1.19	1.68
Added resistance (cmH2O.s/l)	0.53	0.53	0.53	0.54
Added resistance (%)	25.68	22.93	19.10	16.67
Added work of breathing (cmH2O.l)	0.37	0.88	2.95	5.08
Added work of breathing rate (J/min)	0.55	2.20	8.84	17.78
Added work of breathing rate (%)	3.87	5.25	5.52	5.70
N95 FFR				
Level of activity	rest	light activity	moderate activity	heavy activity
Pressure drop - external layer (cmH2O)	0.07	0.14	0.28	0.40
Pressure drop - middle layer (cmH2O)	0.79	1.58	3.16	4.49
Pressure drop - internal layer (cmH2O)	0.02	0.04	0.09	0.12
Pressure drop (cmH2O)	0.88	1.77	3.54	5.01
Added resistance (cmH2O.s/l)	1.59	1.59	1.59	1.59
Added resistance (%)	76.37	68.22	56.83	49.62
Added work of breathing (cmH2O.l)	1.09	2.62	8.79	15.17
Added work of breathing rate (J/min)	1.64	6.56	26.36	53.11
Added work of breathing rate (%)	11.53	15.66	16.48	17.01

Table 5
Effect of wearing surgical masks and N95 respirators with leakage on the pressure drop, resistance, and WOB at different levels of activity.

Surgical mask ($\sigma = 0.05$)				
Level of activity	Rest	Light	Moderate	Heavy
LR	0.080	0.042	.022	0.016
Pressure drop (cmH2O)	0.27	0.57	1.16	1.66
Added resistance (%)	25.68	22.93	19.10	16.67
Added work of breathing rate (%)	3.28	4.82	5.28	5.52
N95 FFR ($\sigma = 0.02$)				
Level of activity	rest	light activity	moderate activity	heavy activity
LR	0.042	0.022	0.011	0.008
Pressure drop (cmH2O)	0.85	1.73	3.50	4.97
Added resistance (%)	76.37	68.21	56.83	49.62
Added work of breathing rate (%)	10.57	14.98	16.11	16.74

Table 6
WOB rate (J/min) in three types of subjects with different lung mechanics at different levels of activity.

Level of activity	Rest	Light	Moderate	Heavy
Healthy lung	14.19	41.88	159.96	312.23
Obstructive lung diseases	22.95	79.13	358.32	795.79
Restrictive lung diseases	21.69	59.88	219.96	415.45

$$k = \frac{d_f^2}{16\alpha\Phi} \quad (5)$$

The modified form of Darcy's equation is Forchheimer's equation that also considers the inertial effects (Eq. (6)) [33].

$$-\nabla P = \frac{\mu}{k}v + \frac{\rho F}{\sqrt{k}}v^2 \quad (6)$$

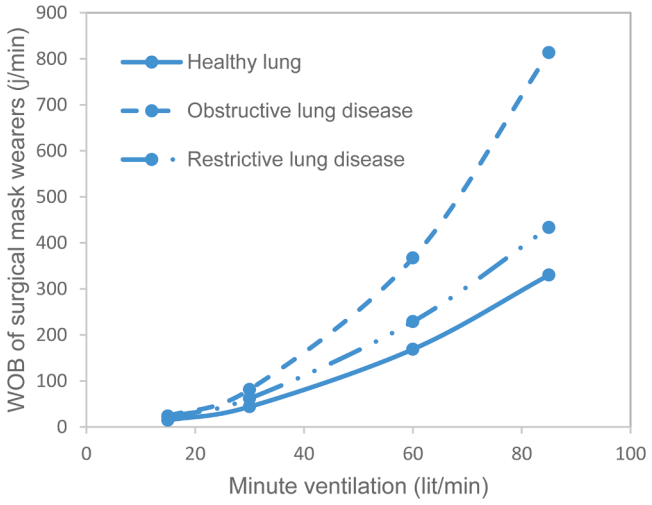

Fig. 3. WOB rate of healthy subjects and patients with obstructive or restrictive lung diseases wearing surgical masks.

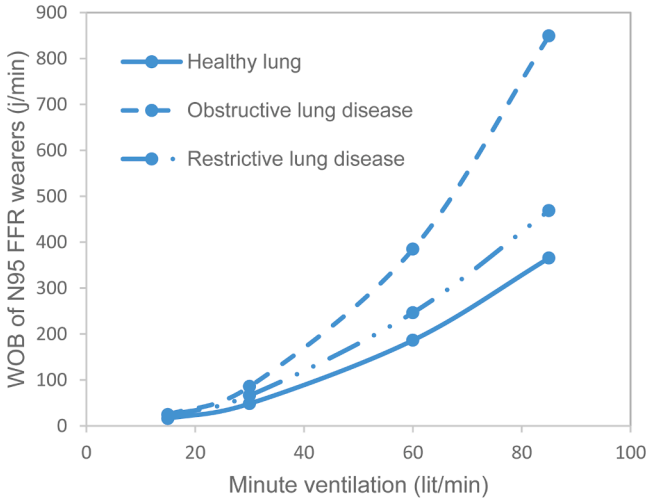

Fig. 4. WOB rate of healthy subjects and patients with obstructive or restrictive lung diseases wearing N95 respirators.

where F is a dimensionless number called Forchheimer coefficient. Ergun suggested another form of Eq. (1) for granular materials expressed by Eq. (7)[34].

$$-\nabla P = \frac{150(1-\varepsilon)^2}{\varepsilon^3 d^2 g}\mu v + \frac{1.75(1-\varepsilon)}{\varepsilon^3 d g}\rho v^2 \tag{7}$$

in which g and d, are gravitational acceleration and fibers diameters, respectively.

According to Eq. (7), F can be expressed by Eq. (8).

$$F = 0.045 / \varepsilon^{3/2} \tag{8}$$

in which ε is the porosity of the fibrous medium. The fibrous masks have multiple layers of randomly nonwoven fibers that are not similar in shape to granular materials. However, there is a good agreement between the F coefficient of Ergun's equation and the numerical data on fibrous structures [34]. So, we have used Eq. (8) for the F coefficient.

In this study, four level of minute ventilation (15, 30, 60, and 85 l/min) were tested which covered the breathing flow rate range of an adult under different activities (rest, light, moderate and heavy activity).

Assuming a sinusoidal profile for the inspiratory flow rate, $f = V_T\pi/(2t_i)\sin(\pi t/t_i)$, the added work of breathing due to mask resistance is computed by Eq. (9)

$$W_{mask} = \int_0^{t_i} f.\Delta p\, dt = \frac{\mu}{k}\frac{L}{A}\frac{t_i}{2}\left(\frac{V_T\pi}{2t_i}\right)^2 + \frac{\rho F}{\sqrt{k}}\frac{L}{A^2}\frac{4t_i}{3}\left(\frac{V_T\pi}{2t_i}\right)^3 \tag{9}$$

In which Δpis the pressure drop due to the mask substituted from the Eq. (6) and t_i, and V_T are the inspiration time and tidal volume, respectively. We have increased the respiratory rate, RR, by increasing the level of activity while I:E = 1:1.1 according to Table 2 [35].

We have computed the basic WOB of the respiratory system by the following equation:

$$WOB = \int_0^{t_i} f.(R_{rs}.f + V/C_{rs})dt = \int_0^{t_i} R_{rs}.f^2 dt + {V_T}^2 \Big/ (2C_{rs}) \tag{10}$$

in which R_{rs}, f, and C_{rs} are the respiratory resistance, inspiratory flow rate, and respiratory compliance. The first term of Eq. (10) is the resistive work required to overcome the frictional resistance to airflow during breathing that occurs due to the resistance of different compartments of the respiratory system, *i.e.* lung airways, and pulmonary and chest wall tissue resistances.

We have compared the values of WOB for three types of lung mechanics, namely healthy, resistive, and obstructive. The compliance values for healthy and obstructive are considered to be 0.1 l/cmH2O, while it is assumed 0.05 l/cmH2O for restrictive lung mechanics. We have followed the previous approach to find respiratory resistance [36]. In this approach, some experimental constants were used for healthy and COPD individuals. The reported constants for COPD individuals are used for obstructive while the constants for both healthy and restrictive lung mechanics are the same.

The porosity and fiber diameter are two parameters that controls both breathability and PFE of the fibrous medium. Increasing the porosity of the fiber medium increase the breathability while could lower the PFE hence it is a double-edged sword.

The PFE may be predicted based on the following formula [37].

$$\eta = 1 - \exp\left(-\frac{4\alpha\eta_f L}{\pi(1-\alpha)d_f}\right) \tag{11}$$

where η_f is the single fiber efficiency due to inertial impaction, η_I, interception, η_R, diffusion, η_D, and adhesion, η_A given in Eq. (12).

$$\eta_f = (\eta_I + \eta_R + \eta_D)\eta_A; \tag{12}$$

In Table 3, the relations for computing these filtration efficiencies by different mechanisms are expressed.

In addition to three main filtration mechanisms, inertial impaction, interception, and diffusion, we could take particle-fiber interaction into account, *i.e.*, the particle rebound and re-entrainment. Eq. (12) calculate the single fiber efficiency based on collision efficiency (sum of collection efficiencies due to impaction, interception, and diffusion) multiplied by the collection efficiency due to adhesion effects [38,39]. According to the formulation of η_A, it is near unity for micron particles in breathing flow rates.

The effect of electrostatic charge of fibers on the filtration efficiency has not been considered in this study. However, the PFE of electret fibers is significantly higher than mechanical ones.

2.1. The effect of leakage flow

In order to consider the leakage flow through the face mask we assume that there is a small gap between mask and face (Fig. 1) [44].

Assuming Darcy's law through the filter material of mask

$$\frac{\Delta P}{L} = -\frac{\mu}{k}v_f \tag{13}$$

Where vf is the face velocity of the filter. Flow through the gap can be

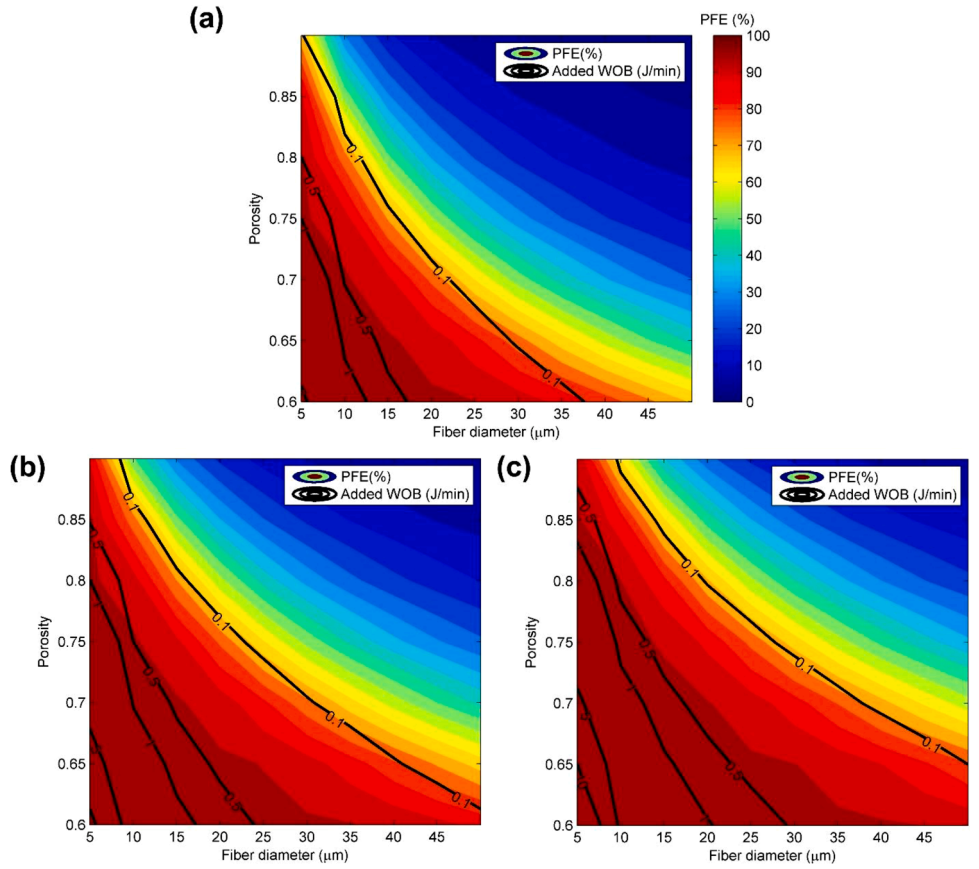

Fig. 5. Added WOB rate (j/min) and PFE (%) for different porosities and fiber diameters in the rest condition assuming a fibrous medium with the thickness of (a) 1 mm, (b) 2 mm, (c) 3 mm.

described with Bernoulli's equation (neglecting the gravitation), with

$$\frac{\Delta P}{\rho}+\frac{{v_g}^2}{2}=0 \tag{14}$$

Where vg is gap air velocity. Combining Eqs. (13) and (14) the relationship between vf and vg can be found, with

$$v_f=\frac{\rho k}{2L\mu}{v_g}^2 \tag{15}$$

The inspiratory flow rate, f, is equal to the volumetric flow rate through the filter, ff, and the gap, fg. So,

$$f=f_f+f_g=A_f v_f+A_g v_g \tag{16}$$

where Af and Ag are the surface area of the filter medium and gap. Substituting Eq. (15) into Eq. (16) yields

$$f=A_f\frac{\rho k}{2L\mu}{v_g}^2+A_g v_g \tag{17}$$

Therefore, vg can be found as below

$$v_g=\frac{-A_g\pm\sqrt{{A_g}^2+2f\frac{A_f\rho k}{L\mu}}}{\frac{A_f\rho k}{L\mu}} \tag{18}$$

It should be noted that this equation has two solutions but only the solution with positive sign is acceptable.

Defining a gap factor, σ=Ag/Af, one can find the leakage flow ratio, LR, as below

$$LR=\frac{f_g}{f}=\frac{f_g}{f_g+f_f}=\frac{A_g v_g}{A_g v_g+A_f v_f}=\frac{\sigma}{\sigma+\frac{v_f}{v_g}}=$$
$$\frac{\sigma}{\sigma+\frac{\rho k}{2L\mu}v_g}=\frac{\sigma}{\sigma+\frac{1}{2A_f}\left(-1+\sqrt{1+2f\frac{\rho k}{\sigma^2 A_f L\mu}}\right)}=\frac{2\sigma A_f}{2\sigma A_f-1+\sqrt{1+2f\frac{\rho k}{\sigma^2 A_f L\mu}}} \tag{19}$$

The normal gap area varies between 0 and 5% of the mask area [44]. We can assume that σ = 0.05 for SMs with large gap and σ = 0.02 for N95 FFRs with small gap.

The inspiratory flow rate, f, substituted in Eq. (8), should be multiplied by (1-LR) to consider the leak flow.

For the PFE calculation, we should also modify the previous PFE, η, as the following equation [44]

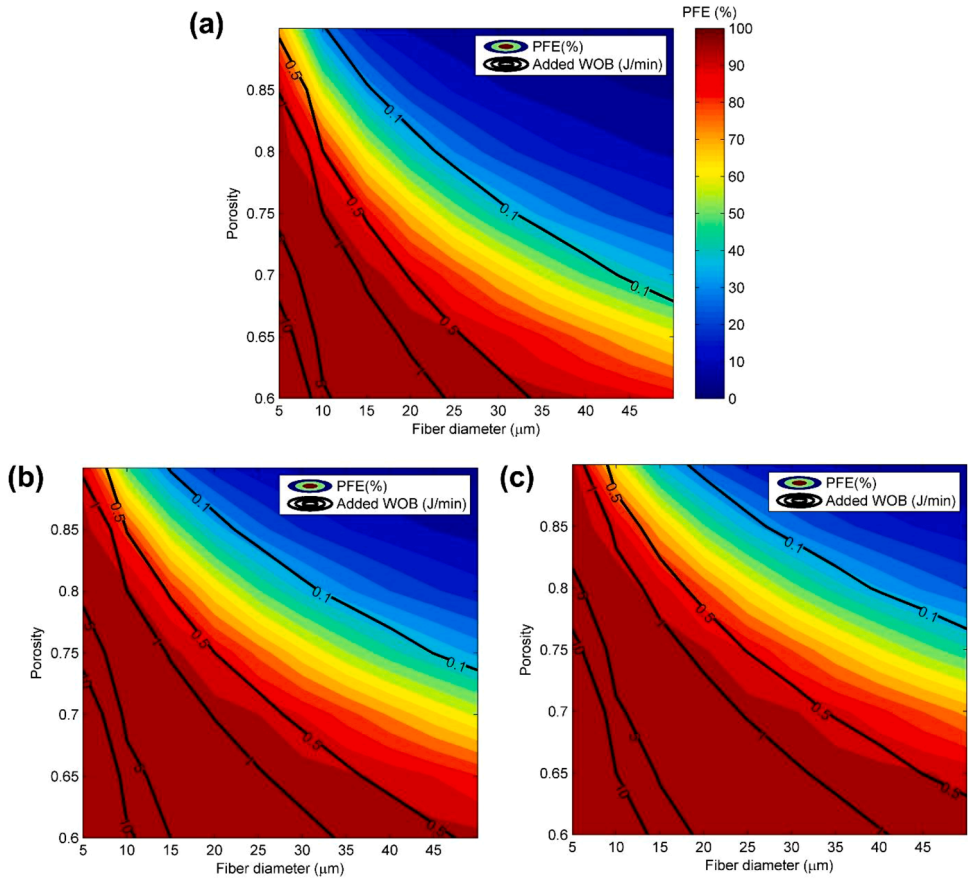

Fig. 6. Added WOB rate (j/min) and PFE (%) for different porosities and fiber diameters in the light activity condition assuming a fibrous medium with the thickness of (a) 1 mm, (b) 2 mm, (c) 3 mm.

$$\eta_{new} = 1 - \left[(1-\eta)\frac{f_f}{f} + \frac{f_g}{f}\right] = 1 - [(1-\eta)(1-LR) + LR] \tag{20}$$

3. Results

3.1. Without leakage flow

The ratio of the second to the first term in the right-hand side of Eq. (6) is shown in Fig. 2. According to Fig. 2, the ratio of the inertial to viscous pressure drop is not significant, even by increasing the flow rate or level of activity in the studied masks. The error caused by ignoring the F coefficient in estimating the pressure drop of the both types of masks is smaller than 1%.

This study computes pressure drop, additional resistance, and WOB imposed on a healthy subject wearing both an SM and an N95 FFR, as shown in Table 4.

3.2. With leakage flow

Assuming that $\sigma = 0.05$ for SMs with large gap and $\sigma = 0.02$ for N95 FFRs with small gap, the leakage ratio, pressure drop, added resistance and WOB are expressed in the Table 5 for different level of activity.

As shown N95 in Table 5, the leakage ratio decreases by increasing inspiratory flow rate consistent with the results of previous research [45]. The comparison of the results in Tables 4 and 5 shows a maximum of 8% decrease in pressure drop and 15% decrease in added WOB under the leakage condition.

According to Table 5, SMs and N95 FFRs cause 0.27 and 0.85 cm H2O pressure drop at rest condition. For the surgical mask, the previously reported pressure drop were 2.667 ± 0.137 mm H2O with the KFDA protocol and 9.283 ± 1.087 mm H2O with the US NIOSH protocol [24]. These two protocols use constant flow rates of 30 and 85 l/min, while our studied flow rates are presented in Table 2. It means that the rest condition (0.56 l/s) is approximately equivalent to tested flow rate of KFDA protocol (30 l/min). Thus, our predicted pressure drop for SMs at rest condition (2.7 mm H2O) well agreed with the measured value at the corresponding flow rate (2.67 mm H2O).

At rest condition, the added resistance is about 25.68 and 76.37% of the healthy lung and the added WOB is about 3.87 and 11.53% of the healthy lung for SMs and N95 FFRs, respectively. The previously reported range for the added inspiratory resistance of N95 FFRs is up to approximately 300% [4,46]. Therefore, our simulation results are within the reasonable range.

In Table 6, the basic values of WOB in the absence of the face mask are computed for subjects with three types of lung mechanics (healthy, obstructive lung disease, and restrictive lung disease). The basic WOB in the diseased lung is about 130–240% of that in the healthy lung and is higher in obstructive lung disease than restrictive lung disease. The total WOB while wearing a mask is shown in Figs. 3 and 4 for healthy and diseased lungs. This increased WOB could be intolerable in patients.

PFE is calculated according to the formulation in the methods section for sodium chloride (used by NIOSH in certification testing of respirators [47]) with the most penetrating particle size (MMPS). The presently accepted MMPs for the mechanical filter (not electret filter) is 0.3 μm [29]. The PFE of external, middle, and internal layers of N95 FFRs for sodium chloride particles at the MPPS at the inhalation flow rate of 30 l/min is 16.99, 79.04, and 5.10%, respectively. Thus, the overall PFE of mechanical N95 FFRs for MPPS at 30 l/min is 1-(1–0.17)(1–0.79)(1–0.05) = 0.83. It is noteworthy that charging fibers in the respirators could increase the PFE of electret respirators above 95% [29].

To investigate the effect of porosity and fiber diameter on the performance of the masks, a one-layer fibrous medium with the known thickness (1, 2, and 3 mm) is assumed. This study computes resistive work imposed by the fibrous medium at rest condition through Eq. (9) for a wide range of porosity and fiber diameter. However, it is not enough because this study aims to keep the PFE above a critical threshold for MPPS. The PFE for different porosities and fiber diameters is computed through Eq. (11). Showing the contours of the added WOB and the PFE in the same plot, one can easily select appropriate ranges of porosity and fiber diameter with desirable added WOB and PFE values. The results are shown in Figs. 5 and 6 for rest and light activity conditions, respectively. The results are shown for three different thicknesses of the fibrous medium (1, 2, and 3 mm).

According to Figs. 5 and 6, to achieve the PFE of mechanical filters above 80% for MPPS, the red region above the line with a determined level of the added WOB is acceptable. As porosity increases, a smaller fiber diameter should be used to obtain the desired level of the PFE and the added WOB. Increasing fiber diameter in a fixed porosity lowers both the added WOB and the PFE. Similarly, increasing porosity in a fixed fiber diameter leads to higher breathability but lower PFE. Increasing the fibrous medium thickness leads to better PFE but lower breathability. According to Fig. 6, increasing the activity level reduces the PFE while increases the added WOB.

4. Discussion

For simplicity, this study assumes that air flows uniformly through the whole surface of the face mask, and there is a uniform pressure in the space between face and mask. However, it is not accurate because the maximum flow is generated just in front of the nose. Therefore, a fluid dynamic analysis for breathing through a face mask covering a human face is suggested as an improvement. Moreover, we have not computed the increase of pressure drop due to the clogging occurred by continuous usage of the face masks. This issue could also increase the added WOB of the wearers in the long durations.

According to Figs. 5 and 6, it is impossible to lower the added WOB while improving the PFE of a face mask by changing the fiber diameter, porosity, and the fibrous medium thickness. So, it is suggested to improve the PFE of the fibrous medium by other techniques such as electrical charging of the fibers.

5. Conclusions

This study examined the effects of face masks on the added resistive WOB of mask wearers at four different levels of physical activity. The added WOB at rest condition was about 3.5% and 11.6% of the healthy lung for SMs and N95 FFRs, respectively. While the body of literature reports that this issue is not significant for healthy individuals, the present study results suggested that face masks may increase WOB, even in healthy individuals during physical activity. Patients with preexisting lung diseases are more likely than healthy individuals to experience increased dyspnea while wearing a face mask due to the increased WOB above their tolerating threshold. This study estimated that using face masks for an extended period of time may increase pressure drop due to clogging.

The simultaneous effects of porosity, fiber diameter, and fibrous medium thickness of a fibrous medium were investigated theoretically on the added WOB and the PFE. Both porosity and fiber diameter can change the added WOB and PFE of face masks. By assuming a constant fiber diameter, a dilute filter with higher porosity has lower added WOB and PFE than a dense filter with lower porosity. Moreover, by assuming a constant porosity, an increase in fiber diameter results in lower added WOB and PFE. Changing the fibrous medium thickness is also a double-edged sword. Thicker filters have better PFE but higher added WOB. We presented these non-linear relations in some contour plots as a quick and simple tool to select the desired values of porosity and fiber diameter in the fibrous medium to ensure that the added WOB is comfortable while the PFE is sufficiently high (Eqs. (4), (17)–(20)).

CRediT authorship contribution statement

Mojdeh Monjezi: Conceptualization, Methodology, Writing – original draft. **Hamidreza Jamaati:** Supervision, Writing – review & editing.

References

[1] Sinkule EJ, Powell JB, Goss FL. Evaluation of N95 respirator use with a surgical mask cover: effects on breathing resistance and inhaled carbon dioxide. Ann Occup Hyg 2013;57:384.
[2] Roberge RJ, Bayer E, Powell JB, Coca A, Roberge MR, Benson SM. Effect of exhaled moisture on breathing resistance of N95 filtering facepiece respirators. Ann Occup Hyg 2010;54:671.
[3] Laird I, Goldsmith R, Pack R, Vitalis A. The effect on heart rate and facial skin temperature of wearing respiratory protection at work. Ann Occup Hyg 2002;46:143.
[4] Lee HP, Wang DY. Objective assessment of increase in breathing resistance of N95 respirators on human subjects. Ann Occup Hyg 2011;55:917.
[5] Roberge RJ, Kim JH, Benson S. N95 filtering facepiece respirator deadspace temperature and humidity. J Occup Environ Hyg 2012;9:166.
[6] Lim E, Seet R, Lee KH, Wilder-Smith E, Chuah B, Ong B. Headaches and the N95 face-mask amongst healthcare providers. Acta Neurol Scand 2006;113:199–202.
[7] Li Y, Tokura H, Guo Y, Wong A, Wong T, Chung J, et al. Effects of wearing N95 and surgical facemasks on heart rate, thermal stress and subjective sensations. Int Arch Occup Environ Health 2005;78:501.
[8] Roberge R, Benson S, Kim JH. Thermal burden of N95 filtering facepiece respirators. Ann Occup Hyg 2012;56:808.
[9] Roberge RJ, Coca A, Williams WJ, Powell JB, Palmiero AJ. Physiological impact of the N95 filtering facepiece respirator on healthcare workers. Respir Care 2010;55:569.
[10] Perna G, Cuniberti F, Daccò S, Nobile M, Caldirola D. Impact of respiratory protective devices on respiration: implications for panic vulnerability during the COVID-19 pandemic. J Affect Disord 2020.
[11] Smith CL, Whitelaw JL, Davies B. Carbon dioxide rebreathing in respiratory protective devices: influence of speech and work rate in full-face masks. Ergonomics 2013;56:781–90.
[12] Roberge RJ, Coca A, Williams WJ, Powell JB, Palmiero AJ. Physiological impact of the N95 filtering facepiece respirator on healthcare workers. Respir Care 2010;55:569–77.
[13] Hopkins SR, Stickland MK, Schoene RB, Swenson ER, Luks AM. Effects of surgical and FFP2/N95 face masks on cardiopulmonary exercise capacity: the numbers do not add up. Clin Res Cardiol 2020;109:1605. official journal of the German cardiac society.
[14] Pan J, Harb C, Leng W, Marr LC. Inward and outward effectiveness of cloth masks, a surgical mask, and a face shield. Aerosol Science and Technology 2021;55:718–33.
[15] Crilley LR, Angelucci AA, Malile B, Young CJ, VandenBoer TC, Chen JIL. Non-woven materials for cloth-based face masks inserts: relationship between material properties and sub-micron aerosol filtration. Environ Sci Nano 2021;8:1603.
[16] Long KD, Woodburn EV, Berg IC, Chen V, Scott WS. Measurement of filtration efficiencies of healthcare and consumer materials using modified respirator fit tester setup. PLoS ONE 2020;15:e0240499.
[17] Zangmeister CD, Radney JG, Vicenzi EP, Weaver JL. Filtration efficiencies of nanoscale aerosol by cloth mask materials used to slow the spread of SARS-CoV-2. ACS Nano 2020;14:9188.
[18] Zhao M, Liao L, Xiao W, Yu X, Wang H, Wang Q, et al. Household materials selection for homemade cloth face coverings and their filtration efficiency enhancement with triboelectric charging. Nano Lett 2020;20:5544.
[19] Konda A, Prakash A, Moss GA, Schmoldt M, Grant GD, Guha S. Aerosol filtration efficiency of common fabrics used in respiratory cloth masks. ACS Nano 2020;14:6339.
[20] Ou Q, Pei C, Chan KS, Abell E, Pui DYH. Evaluation of decontamination methods for commercial and alternative respirator and mask materials – view from filtration aspect. J Aerosol Sci 2020;150:105609.
[21] Podgórski A, Bałazy A, Gradoń L. Application of nanofibers to improve the filtration efficiency of the most penetrating aerosol particles in fibrous filters. Chem Eng Sci 2006;61:6804.
[22] Drewnick F, Pikmann J, Fachinger F, Moormann L, Sprang F, Borrmann S. Aerosol filtration efficiency of household materials for homemade face masks: influence of material properties, particle size, particle electrical charge, face velocity, and leaks. Aerosol Sci Technol 2020;55:1–17.
[23] Grinshpun SA, Haruta H, Eninger RM, Reponen T, McKay RT, Lee SA. Performance of an N95 filtering facepiece particulate respirator and a surgical mask during human breathing: two pathways for particle penetration. J Occup Environ Hyg 2009;6:593–603.
[24] Jung H, Kim JK, Lee S, Lee J, Kim J, Tsai P, et al. Comparison of filtration efficiency and pressure drop in anti-yellow sand masks, quarantine masks, medical masks, general masks, and handkerchiefs. Aerosol Air Qual Res 2013;14:991–1002.

[25] Dbouk T, Drikakis D. On respiratory droplets and face masks. Phys Fluids 1994; 2020(32):063303.
[26] Tcharkhtchi A, Abbasnezhad N, Zarbini SM, Zirak N, Farzaneh S, Shirinbayan M. An overview of filtration efficiency through the masks: mechanisms of the aerosols penetration. Bioact Mater 2021;6:106.
[27] Whitaker S. Flow in porous media I: a theoretical derivation of Darcy's law. Transp Porous Media 1986;1:3–25.
[28] Leonas KK, Jones CR, Hall D. The relationship of fabric properties and bacterial filtration efficiency for selected surgical face masks. J Text Appar Technol Manag 2003;78:1–8.
[29] Balazy A, Toivola M, Reponen T, PodgÓRski A, Zimmer A, Grinshpun SA. Manikin-based performance evaluation of N95 filtering-facepiece respirators challenged with nanoparticles. Ann Occup Hyg 2006;50:259.
[30] Ramirez JA, O'Shaughnessy PT. The effect of simulated air conditions on N95 filtering facepiece respirators performance. J Occup Environ Hyg 2016;13: 491–500.
[31] Rengasamy S, Miller A, Eimer BC, Shaffer RE. Filtration performance of FDA-cleared surgical masks. J Int Soc Respir Prot 2009;26:54–70.
[32] Spielman L, Goren SL. Model for predicting pressure drop and filtration efficiency in fibrous media. Environ Sci Technol 1968;2:279.
[33] Firoozabadi A, Katz DL. An analysis of high-velocity gas flow through porous media. J Pet Technol 1979;31:211.
[34] Tamayol A. Micro/macroscopic fluid flow in open cell fibrous structures and porous media. Simon Fraser University; 2011.
[35] Neder JA, Dal CS, Malaguti C, Reis S, De Fuccio MBd, Schmidt H, et al. The pattern and timing of breathing during incremental exercise: a normative study. Eur Respir J 2003;21:530.
[36] Monjezi M, Jamaati H. The effects of pressure-versus volume-controlled ventilation on ventilator work of breathing. Biomed Eng Online 2020;19:1–14.
[37] Bulejko P. Numerical comparison of prediction models for aerosol filtration efficiency applied on a hollow-fiber membrane pore structure. Nanomaterials 2018;8:447 (Basel).
[38] Maddineni AK, Das D, Damodaran RM. Air-borne particle capture by fibrous filter media under collision effect: a CFD-based approach. Sep Purif Technol 2018;193: 1–10.
[39] Kasper G, Schollmeier S, Meyer J, Hoferer J. The collection efficiency of a particle-loaded single filter fiber. J Aerosol Sci 2009;40:993–1009.
[40] Zhu C, Lin CH, Cheung CS. Inertial impaction-dominated fibrous filtration with rectangular or cylindrical fibers. Powder Technol 2000;112:149.
[41] Kirsch M, Stechkina I. Fundamentals of aerosol science: the theory of aerosol filtration with fibrous filters. New York: John Wiley & Sons; 1978.
[42] Stechkina IB, Kirsch AA, Fuchs NA. Studies on fibrous aerosol filters-IV calculation of aerosol deposition in model filters in the range of maximum penetration. Ann Occup Hyg 1969;12:1–8.
[43] Ptak T, Jaroszczyk T. Theoretical-experimental aerosol filtration model for fibrous filters at intermediate reynolds numbers. In: Proceedings of the 5th world filtration congress; 1990. p. 5–8. Nice, France.
[44] Xu M, Lee P, Collins D. The critical importance of mask seals on respirator performance: an analytical and simulation approach. PLoS ONE 2021;16: e0246720.
[45] Lei Z, Yang J, Zhuang Z, Roberge R. Simulation and evaluation of respirator faceseal leaks using computational fluid dynamics and infrared imaging. Ann Occup Hyg 2013;57:493–506.
[46] Zhang X, Li H, Shen S, Cai M. Investigation of the flow-field in the upper respiratory system when wearing N95 filtering facepiece respirator. J Occup Environ Hyg 2016;13:372.
[47] NIOSH. 42 CFR Part 84: respiratory protective devices. Title 42 Code of Federal Regulations Ch. I (10–1–97 Edition).